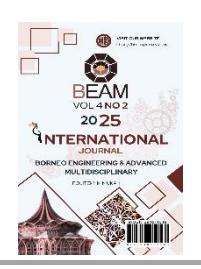


Borneo Engineering & Advanced Multidisciplinary International Journal (BEAM)

Volume 4, Issue 2, November 2025, Pages 29-34



3D Printing of Bioactive PLA/PA12/WA Composites: Toward High-Performance Bone Implant Materials

Nur Munirah Mustaza¹, Farrahshaida Mohd Salleh^{1*}, Muhammad Hussain Ismail¹, Izdihar Tharazi¹, Abdul Manaf Abdullah¹

¹Faculty of Mechanical Engineering, Universiti Teknologi MARA, 40450 Shah Alam, Selangor, Malaysia

*Corresponding author: fshaida@uitm.edu.my

Please provide an official organisation email of the corresponding author

Full Paper

Article history
Received
30 June 2025
Received in revised form
27 August 2025
Accepted
8 October 2025
Published online
1 November 2025



Abstract

Bone implantation is among the most performed tissue transplantation procedures globally, particularly in cases involving severe clinical conditions such as bone trauma, tumors, cystic lesions, and high-impact injuries. However, traditional fabrication methods are often associated with several clinical complications, including a heightened risk of infection, excessive intraoperative bleeding, and potential implant failure due to fracture. To overcome these limitations, additive manufacturing techniques, particularly fused deposition modelling (FDM) using polymer-ceramic hybrid composites, have emerged as promising alternatives for fabricating bone grafts. In this study, a composite consisting of polylactic acid (PLA), polyamide 12 (PA12), and wollastonite (WA) in a 60PLA/40Pwt%PA12 with10wt%WA formulation was meltcompounded using a twin-screw extruder at temperatures ranging from 185 to 200 °C. Filaments were successfully fabricated with a consistent diameter of 1.7 ± 0.2 mm under optimized conditions (extrusion temperature: 200–205 °C; screw speed: 3 rpm; cooling fan speed: 50). Cylindrical and cuboid specimens were fabricated via fused deposition modelling (FDM) using printing temperatures ranging from 200 °C to 220 °C, layer heights between 0.1 mm and 0.3 mm, a constant print speed of 50 rpm, and infill densities of 100%. The printed samples were subjected to physical characterization namely density measurement using the Archimedes principle and mechanical evaluation through vickers hardness and compression testing. Finding shows that, vickers hardness of 18.7 HV was recorded at a printing temperature of 200 °C with a layer height of 0.1 mm. This same parameter set also yielded the highest compressive strength of 146.71 MPa, a compressive modulus of 1.52 GPa, and an ultimate strain of 67.94%, demonstrating mechanical characteristics closely aligned with those of natural cancellous bone. These results highlight that lower layer heights, combined with an optimized printing temperature of 200 °C, enhance the printability and mechanical performance of the 60PLA/40PA12/10WA composite filament, suggesting strong potential for future application in bone implant fabrication due to its favourable structural and functional properties.

Keywords: - Polylactic acid/Polyamide 12/Wollastonite composite, fused deposition modelling, density, vickers hardness, compression test

Copyright © This is an open access article distributed under the terms of the Creative Commons Attribution License



1. Introduction

The global 3D printing market was valued at USD 17.5 billion in 2024 and is projected to reach USD 37.4 billion by 2029, growing at a compound annual growth rate (CAGR) of 16.4% (Global 3D Printing Market Size, Share, Trends & Growth Analysis 2032, n.d.). This rapid market expansion underscores the widespread adoption of 3D

printing technologies across various industries, including the biomedical sector. The growing interest in this technology is largely attributed to its user-friendly nature, cost-effectiveness, reduced fabrication time, and the ability to produce customized products. In biomedical applications, 3D printing has garnered significant attention from researchers due to its flexibility in design and ease of fabrication. It has been employed in the development of medical devices (e.g., screws, sutures), tissue engineering

scaffolds, drug delivery systems, and more. Specifically in the context of bone implantation, 3D printing has been extensively studied and applied, owing to its ability to provide precise control over scaffold architecture, including tunable porosity and interconnected structures that promote cell proliferation, tissue integration, and improved mechanical performance (Wang et al., 2021). This technology is particularly suitable for addressing critical-size bone defects typically bigger than 2.5 cm, which require bone implant scaffolds for effective regeneration (Shah et al., 2023). Compared to conventional approaches such as allografts and xenografts, which are often associated with limitations including graft rejection, high cost, bleeding complications, and risk of disease transmission thus, 3D printing offers a safer and more efficient alternative (Srinath et al., 2020). Traditional methods in bone tissue engineering, such as solvent casting and salt-leaching, have become less relevant due to their inability to provide sufficient porosity for vascularization and their inadequate structural integrity (Ansari et al., 2024). Therefore, this study adopts a fused deposition modeling (FDM) approach, which utilizes a layer-by-layer technique with filament-based feedstocks to fabricate 3D lattice scaffolds. This method enables the design of internal porous structures to support biological growth factors, while offering a cost-effective and time-efficient fabrication process.

Polylactic acid (PLA) is a widely used material in bone tissue engineering, primarily due to its biodegradability and bio-based origin. It is derived from renewable resources such as sugarcane, corn starch, and tapioca roots through polymerization processes, and is also produced on a large scale via bioconversion techniques (Chaiwutthinan et al., 2019). Furthermore, PLA degrades environmentally benign by-products, contributing to its recognition as a safe material. As a result, PLA has received approval from the U.S. Food and Drug Administration (FDA) for various biomedical applications . Its mechanical toughness has made it attractive for use in medical devices, including orthopedic and dental fixation components such as screws and washers (Chen et al., 2019). However, PLA is inherently brittle and exhibits poor ductility, which limits its application in load-bearing scenarios (Saravana & Kandaswamy, 2019). Additionally, PLA demonstrates weak biological activity, resulting in suboptimal cellular responses when used as a bone substitute (Esposito Corcione et al., 2017). To overcome its mechanical limitations, polyamide 12 (PA12) has been incorporated into PLA to form a biphasic polymer composite with improved toughness and flexibility. PA12 is known for its excellent wear resistance, flexibility, and stiffness, making it a suitable candidate for enhancing the performance of PLA-based matrices. Raj et al. (2020) reported on PLA/PA12 composites with varying PA12 contents (10-40 wt%), showing that a 40 wt% PA12 addition led to a brittle-to-ductile transition, with elongation at break reaching up to 170%, significantly higher than that of the lower PA12 content blends (Raj et al., 2020). However, studies have demonstrated that increasing PA12 content beyond 50 wt% results in a decline in mechanical strength (Murariu et al., 2023). Despite the enhanced mechanical performance, PLA/PA12

composites still lack sufficient bioactivity required for bone regeneration. To address this, wollastonite (WA), a bioactive ceramic, is incorporated into the PLA matrix to impart essential properties such as osteoconductivity, cell proliferation support, and bone tissue regeneration (Shie et al., 2017). WA also provides antibacterial effects against clinical pathogens and contributes to pH buffering during PLA degradation by neutralizing acidic by-products, thus minimizing inflammation risks (Goswami et al., 2013 & Venkatraman et al., 2021).

In this study, a 60PLA/40PA12/10WA composite was prepared via melt blending using a twin-screw extruder to ensure uniform dispersion and homogenization of the polymer-ceramic system. The composite filament was subsequently produced with a diameter of 1.75 ± 0.2 mm using a filament extrusion machine. The 3D printing process was performed using varying temperatures, layer thicknesses, and infill densities to evaluate the composite's physical and mechanical properties, with the aim of determining its suitability for bone implant applications.

2. Methodology

2.1 Preparation of Composite Materials

The raw materials were measured according to their weight percentages to prepare a composite feedstock, consisting of 60 wt% PLA, 40 wt% PA12, and 10 wt% WA ceramic powder. All raw materials, PLA pellets, PA12 powder, and WA were pre-dried in a convection oven at 50 °C for 24 hours. Each material was covered with perforated aluminium foil to ensure even moisture removal and to prevent pressure build-up from heated air within the containers.

For the pre-mixing stage, all dried materials were combined in a single container and manually blended using a spatula to achieve a uniform physical mixture. The pre-mixed composite was then processed using a Prism 16 mm twin-screw extruder equipped with four heating zones set at 185 °C, 190 °C, 195 °C, and 200 °C, respectively. The torque was carefully monitored and maintained below 50%, as values exceeding this threshold trigger an automatic shutdown of the machine.

Upon extrusion, the molten composite was flattened into sheets to facilitate cooling and prevent clogging during subsequent processing. Once cooled, the sheets were granulated using a jaw crusher. The resulting granules were stored in double-sealed plastic bags with silica gel packets to prevent moisture absorption.

2.2 Filament Fabrication

The composite granules were dried overnight at 55 °C in aluminium trays before filament production to eliminate any residual moisture. The dried granules were then processed using the 3DEVO Filament Maker Precision system. The extrusion temperatures across the four heating zones were set to 205 °C, 210 °C, 210 °C, and 205 °C, respectively. The screw speed was maintained at a moderate rate, with a cooling fan operating at 50% speed. The produced filament achieved a consistent

diameter of 1.75 ± 0.2 mm. After extrusion, the spooled filament was stored in double-sealed plastic bags with silica gel to maintain dryness.



Fig. 1: 60PLA/40PA12/10WA composite filament

2.3 3D Printing Process

Cuboid specimens (10 mm length and width × 5 mm thickness) were printed for Vickers hardness testing, while cylindrical specimens of the 60PLA/40PA12/10WA composite (12 mm height × 6 mm diameter) were fabricated for compressive testing. All samples were produced using an Ender 6 FDM 3D printer. The cylindrical design was created using CATIA software and converted into G-code using Ultimaker Cura slicing software. To evaluate the influence of process parameters, three extrusion temperatures (200 °C, 210 °C, and 220 °C), three-layer height (0.1 mm, 0.2 mm, and 0.3 mm), and three infill densities (60%, 80%, and 100%) were investigated. A fixed printing speed of 50 rpm and a linear infill pattern were consistently applied across all printing conditions.





Fig. 2: Printed sample of (a)cylindrical shape and (b) cuboid shape

2.4 Physical and Mechanical Characterization

The printed specimens were evaluated for their physical and mechanical properties. Density measurements were carried out using the Archimedes principal ASTM D792, by using corn oil (density = 0.925 g/cm³) as the immersion medium. Vickers hardness test according to ASTM E384 was carried out using a Mitutoyo Vickers hardness tester machine with a 1 kgfa Mitutoyo Vickers hardness tester machine with a 1 kgf load cell and a 10-second indentation.

Compressive strength testing was conducted following ASTM D695 using a Shimadzu Universal Testing Machine with a 100 kN load capacity and a 1 mm/min crosshead speed at room temperature.

3. Result and Discussion

3.1 Density Analysis

Density measurements were conducted to assess the homogeneity of the 60PLA/40PA12/10WA composite blend. The theoretical density of the composite was calculated using the rule of mixtures based on the individual densities of the constituent materials, PLA, PA12, and wollastonite WA which were determined via helium gas pycnometry. The resulting theoretical density of composite was 1.205 g/cm³, as shown in Table 1. Meanwhile, the actual density of the 3D-printed specimens was measured using the Archimedes principle, with the corresponding results presented in Table 2. The composite exhibited a slightly lower density of 1.18 g/cm³ compared to neat PLA (1.22 g/cm³), a difference attributable to the incorporation of PA12, which has a lower intrinsic density (1.01 g/cm³), thereby reducing the overall density of the composite system. The density deviation between the theoretical and experimental values was approximately 2%, suggesting good dispersion and homogeneity within the composite matrix.

Notably, specimens fabricated with a lower layer height of 0.1 mm exhibited minimal deviation, whereas those printed with larger layer heights (0.3 mm) showed increased discrepancies, irrespective of the printing temperature. These observations underscore the critical influence of layer height on density uniformity. A reduced layer height promotes finer material deposition and stronger interlayer adhesion, thereby minimizing void formation and enhancing structural cohesion. In contrast, larger layer heights tend to result in incomplete fusion between layers, increased porosity, and consequently, lower bulk density, which compromises the mechanical integrity of the printed parts (Mazlan et al., 2023). The density showed by 60PLA/40PA12/10WA composite and printed part is in the range of native bone density (Ramli et al., 2024).

Table 1: Density analysis of raw materials and composite

| Material | Theoretica l density (g/cm³) | Experimenta I density (g/cm³) | Percentag e error (%) |
|---------------------------------|------------------------------------|-------------------------------------|-----------------------------|
| PLA pellet | 1.24 | 1.220 | 1.61 |
| PA12 powder | 1.01 | 1.031 | 1.98 |
| WA powder | 2.90 | 2.647 | 8.62 |
| 60PLA/40PA12/10W A composite | 1.205 | 1.180 | 2.07 |

Table 2: Density analysis of 60PLA/40PA12/10WA composite printed part

| Printing temperature (°C) | Infill density (%) | Layer height (mm) | Experimental density (g/cm³) | Percentage error (%) |
|---------------------------------|--------------------------|-------------------------|------------------------------|-------------------------|
| 200 | 100 | 0.1 | 1.202 | 0.22 |
| | | 0.3 | 1.100 | 8.71 |
| 210 | 100 | 0.2 | 1.205 | 0 |
| 220 | 100 | 0.1 | 1.203 | 0.15 |
| | | 0.3 | 1.188 | 1.38 |

3.2 Vickers Hardness Test

The Vickers hardness values obtained from Table 3 indicate a strong dependence on layer height, with lower heights producing superior surface hardness. At a printing temperature of 200 °C, decreasing the layer height from 0.3 mm to 0.1 mm increased the hardness from 14.9 HV to 18.7 HV, the highest value observed across all conditions. This trend can be attributed to improved interlayer diffusion and reduced porosity at smaller layer heights, which result in denser and more homogeneously consolidated material at the surface. A similar trend was observed at 220 °C, where the Vickers hardness decreased from 15.7 HV at a 0.1 mm layer height to 14.3 HV at 0.3 mm, further emphasizing the influence of finer layer deposition in enhancing surface consolidation. This observation aligns with previous studies reporting that increased layer thickness adversely affects hardness due to interlayer bonding and higher surface reduced irregularities (Shubham et al., 2016).At 210 °C and 0.2 mm, the measured hardness of 16.1 HV lies intermediate between the 0.1 mm and 0.3 mm cases, consistent with the expected improvement in bonding as layer thickness is reduced. Bigger layer height tends to create pore formation between layers due to poor adhesion layer and promote crack initiation (Zhang et al., 2024). The overall decline in hardness at elevated temperatures, despite finer layer height, can be explained by the onset of thermal softening or minor degradation of PLA, which becomes thermally sensitive beyond 210 °C. These results collectively confirm that finer layer resolution (particularly 0.1 mm) enhances surface hardness by reducing interlayer gaps and improving polymer chain entanglement across layers.

Table 3: Vickers hardness of 60PLA/40PA12/10WA composite printed part

| Printing temperature (°C) | Infill density (%) | Layer height (mm) | Hardness (HV) |
|---------------------------------|--------------------|-------------------|------------------|
| 200 | 100 | 0.1 | 18.7 |
| | | 0.3 | 14.9 |
| 210 | 100 | 0.2 | 16.1 |
| 220 | 100 | 0.1 | 15.7 |
| | | 0.3 | 14.3 |

3.3 Compression Test

Compression test results in Table 4 further validate the beneficial effect of low layer height and optimal temperature on bulk mechanical performance. At 200 °C and 0.1 mm, the composite demonstrated its highest compressive strength $(146.71 \pm 9.72 \text{ MPa})$, modulus $(1.52 \pm 0.15 \text{ GPa})$, and a high ultimate $(67.94 \pm 1.49\%)$. These values reflect superior loadbearing capability and toughness, properties essential for bone implant applications (Gerhardt & Boccaccini, 2010). The mechanical advantage at this condition is likely due to optimal melt viscosity, enhanced filler dispersion, and efficient interlayer fusion, which reduce structural defects and enable better stress transfer through the material. As the layer height increased to 0.3 mm under the same temperature, the strength drastically decreased to 35.03 ± 5.2 MPa, the modulus dropped to 0.52 ± 0.07 GPa, and the strain fell to $18.01 \pm 2.12\%$. This significant reduction suggests poor interlayer bonding and increased porosity at thicker layers, which act as failure initiation points under compressive loads. The drop in performance aligns with the known effects of large layer heights, reducing effective bonding area and increasing geometric inaccuracy, which compromises structural integrity (Xu et al., 2021).

Table 4: Compression test data of 60PLA/40PA12/10WA composite printed part

| Printing Temperature (°C) | Infill Density (%) | Layer Height (mm) | Compressive Strength (MPa) | Compressive Modulus (GPa) | Ultimate Strain (%) |
|------------------------------|--------------------|----------------------|----------------------------|------------------------------|---------------------|
| 200 | 100 | 0.1 | 146.71 ± 9.72 | 1.52 ± 0.15 | 67.94 ± 1.49 |
| | - | 0.3 | 35.03 ± 5.2 | 0.52 ± 0.07 | 18.01 ± 2.12 |
| 210 | 100 | 0.2 | 107.52 ± 25.13 | 1.07 ± 0.13 | 72.00 ± 2.93 |
| 220 | 100 | 0.1 | 109.36 ± 23.32 | 1.59 ± 0.20 | 53.46 ± 19.97 |
| | _ | 0.3 | 50.82 ± 10.23 | 0.89 ± 0.31 | 16.27 ± 2.57 |

At $210\,^{\circ}\text{C}$ and $0.2\,\text{mm}$, a compressive strength of $107.52\pm25.13\,\text{MPa}$ and the highest strain value of $72.00\pm2.93\%$ were observed. This suggests an improved ductile response and a favourable balance between flowability and adhesion, possibly due to better thermal softening of PA12, which enhances interfacial compatibility with PLA. At $220\,^{\circ}\text{C}$ and $0.1\,\text{mm}$, the

compressive strength remained high $(109.36 \pm 23.32 \text{ MPa}),$ and modulus peaked 1.59 ± 0.20 GPa. Conversely, the condition of 220 °C and 0.3 mm vielded relatively low strength $(50.82 \pm 10.23 \text{ MPa})$, modulus $(0.89 \pm 0.31 \text{ GPa})$, and the lowest strain $(16.27 \pm 2.57\%)$ among all samples. This reflects the cumulative negative effect of excessive temperature and thick layer deposition, both of which degrade interlayer fusion and microstructural integrity, leading to a weakened compressive response.

4. Conclusion and Recommendations

Therefore, the printing parameters of 200 °C, 0.1 mm layer height, and 100% infill density represent the most suitable combination for achieving the desired mechanical properties, which include good density, high surface hardness, compressive strength, modulus, and ductility due to enhanced deposition resolution, minimized porosity, and stronger interfacial bonding. Meanwhile, 200 °C is the optimal printing temperature, balancing melt flow and material integrity without causing thermal degradation. These attributes are essential for the structural demands of load-bearing bone implants.

Acknowledgement: The acknowledgement is given to Universiti Teknologi MARA (UiTM) for financial support under Geran Insentif Penyeliaan (Project File No. RD/47/002/2025) and providing laboratory facilities.

Author Contributions: The research study was carried out successfully with contributions from all authors.

Conflicts of Interest: The authors declare no conflict of interest.

References

Ansari, M. A. A., Makwana, P., Dhimmar, B., Vasita, R., Jain, P. K., & Nanda, H. S. (2024). Design and development of 3D printed shape memory triphasic polymer-ceramic bioactive scaffolds for bone tissue engineering. *Journal of Materials Chemistry B*, *12*(28), 6886–6904.

https://doi.org/10.1039/d4tb00785a.

Chaiwutthinan, P., Chuayjuljit, S., Srasomsub, S., & Boonmahitthisud, A. (2019). Composites of poly(lactic acid)/poly(butylene adipate-co-terephthalate) blend with wood fiber and wollastonite: Physical properties, morphology, and biodegradability. *Journal of Applied Polymer Science*, 136(21).

https://doi.org/10.1002/app.47543.

Chen, X., Gao, C., Jiang, J., Wu, Y., Zhu, P., & Chen, G. (2019). 3D printed porous PLA/nHA composite scaffolds with enhanced osteogenesis and osteoconductivityin vivo for bone regeneration. *Biomedical Materials (Bristol)*, 14(6).

https://doi.org/10.1088/1748-605X/ab388d.

Esposito Corcione, C., Gervaso, F., Scalera, F., Montagna, F., Sannino, A., & Maffezzoli, A. (2017). The feasibility of printing polylactic acidnanohydroxyapatite composites using a low-cost fused deposition modeling 3D printer. *Journal of Applied Polymer Science*, 134(13).

https://doi.org/10.1002/app.44656.

Gerhardt, L. C., & Boccaccini, A. R. (2010). Bioactive glass and glass-ceramic scaffolds for bone tissue engineering. *Materials*, *3*(7), 3867–3910. https://doi.org/10.3390/MA3073867.

- Global 3D Printing Market Size, Share, Trends & Growth Analysis 2032. (n.d.). Retrieved May 26, 2025, from https://www.marketsandmarkets.com/Market-Reports/3d-printing-market-1276.html.
- Goswami, J., Bhatnagar, N., Mohanty, S., & Ghosh, A. K. (2013). Processing and characterization of poly(lactic acid) based bioactive composites for biomedical scaffold application. *Express Polymer Letters*, 7(9), 767–777.

https://doi.org/10.3144/expresspolymlett.2013.74.

Mazlan, M. A., Anas, M. A., Nor Izmin, N. A., & Abdullah, A. H. (2023). Effects of Infill Density, Wall Perimeter and Layer Height in Fabricating 3D Printing Products. *Materials* 2023, Vol. 16, Page 695, 16(2), 695

https://doi.org/10.3390/MA16020695.

- Murariu, M., Arzoumanian, T., Paint, Y., Murariu, O., Raquez, J. M., & Dubois, P. (2023). Engineered polylactide (PLA)—polyamide (PA) blends for durable applications: 1. PLA with high crystallization ability to tune up the properties of PLA/PA12 blends. *European Journal of Materials*, 3(1), 1–36. https://doi.org/10.1080/26889277.2022.2113986.
- Raj, A., Prashantha, K., & Samuel, C. (2020). Compatibility in biobased poly(L-lactide)/polyamide binary blends: From melt-state interfacial tensions to (thermo)mechanical properties. *Journal of Applied Polymer Science*, *137*(10). https://doi.org/10.1002/app.48440.
- Ramli, M. I., Choudhury, A. M., Choong, D. L. J., Jie Jun, T., Rajendran Royan, N. R., & Meor Tajudin, M. A. F. (2024). PLA/Wollastonite Composite Filaments for 3D Printing Application: Rheological Properties and Extrusion. *Jurnal Kejuruteraan*, *36*(5), 2097–2106. https://doi.org/10.17576/jkukm-2024-36(5)-26.
- Saravana, S., & Kandaswamy, R. (2019). Investigation on the Mechanical and Thermal Properties of PLA/Calcium Silicate Biocomposites for Injection Molding Applications. *Silicon*, *11*(2), 1143–1150. https://doi.org/10.1007/s12633-018-9926-9.
- Shah, F. A., Jolic, M., Micheletti, C., Omar, O., Norlindh, B., Emanuelsson, L., Engqvist, H., Engstrand, T., Palmquist, A., & Thomsen, P. (2023). Bone without borders Monetite-based calcium phosphate guides bone formation beyond the skeletal envelope. *Bioactive Materials*, *19*, 103–114. https://doi.org/10.1016/J.BIOACTMAT.2022.03.012.
- Shie, M. Y., Chiang, W. H., Chen, I. W. P., Liu, W. Y., & Chen, Y. W. (2017). Synergistic acceleration in the osteogenic and angiogenic differentiation of human mesenchymal stem cells by calcium silicate—graphene composites. *Materials Science and Engineering: C*, 73, 726–735.

https://doi.org/10.1016/J.MSEC.2016.12.071.

- Shubham, P., Sikidar, A., & Chand, T. (2016). The influence of layer thickness on mechanical properties of the 3D printed ABS polymer by fused deposition modeling. *Key Engineering Materials*, 706, 63–67. https://doi.org/10.4028/WWW.SCIENTIFIC.NET/KEM.706.63.
- Srinath, P., Abdul Azeem, P., & Venugopal Reddy, K. (2020). Review on calcium silicate-based bioceramics in bone tissue engineering. *International Journal of Applied Ceramic Technology*, 17(5), 2450–2464. https://doi.org/10.1111/ijac.13577.
- Venkatraman, S. K., Choudhary, R., Genasan, K., Murali, M. R., Raghavendran, H. R. B., Kamarul, T., Suresh, A., Abraham, J., Venkateswaran, S., Livingston, A., & Swamiappan, S. (2021). Antibacterial wollastonite supported excellent proliferation and osteogenic differentiation of human bone marrow derived mesenchymal stromal cells. *Journal of Sol-Gel Science and Technology*, 100(3), 506–516.
- Wang, W., Zhang, B., Li, M., Li, J., Zhang, C., Han, Y., Wang, L., Wang, K., Zhou, C., Liu, L., Fan, Y., & Zhang, X. (2021). 3D printing of PLA/n-HA composite scaffolds with customized mechanical properties and biological functions for bone tissue engineering. *Composites Part B: Engineering*, 224. https://doi.org/10.1016/j.compositesb.2021.109192.
- Xu, Q., Jiang, L., Ma, C., Niu, Q., & Wang, X. (2021). Effect of Layer Thickness on the Physical and Mechanical Properties of Sand Powder 3D Printing Specimens. *Frontiers in Earth Science*, 9, 763202. https://doi.org/10.3389/FEART.2021.763202/BIBTE X.
- Zhang, L., Wang, M., Li, H., Li, Q., & Liu, J. (2024). Influence of layer thickness and heat treatment on microstructure and properties of selective laser melted maraging stainless steel. *Journal of Materials Research and Technology*, *33*, 3911–3927. https://doi.org/10.1016/J.JMRT.2024.10.097.